Development 129, 4821-4830 (2002)
Printed in Great Britain © The Company of Biologists Limited 2002
DEV0447

Mutant alleles of *Arabidopsis RADIALLY SWOLLEN 4* and *7* reduce growth anisotropy without altering the transverse orientation of cortical microtubules or cellulose microfibrils

Allison M. D. Wiedemeier[1], Jan E. Judy-March[1], Charles H. Hocart[2], Geoffrey O. Wasteneys[2], Richard E. Williamson[2] and Tobias I. Baskin[1,*]

[1]Division of Biological Sciences, University of Missouri, Columbia, Missouri 65211-7400, USA
[2]Plant Cell Biology Group, Research School of Biological Sciences, Australian National University, Canberra ACT 2601, Australia
*Author for correspondence (e-mail: BaskinT@missouri.edu)

Accepted 22 July 2002

SUMMARY

The anisotropic growth of plant cells depends on cell walls having anisotropic mechanical properties, which are hypothesized to arise from aligned cellulose microfibrils. To test this hypothesis and to identify genes involved in controlling plant shape, we isolated mutants in *Arabidopsis thaliana* in which the degree of anisotropic expansion of the root is reduced. We report here the characterization of mutants at two new loci, *RADIALLY SWOLLEN 4 (RSW4)* and *RSW7*. The radial swelling phenotype is temperature sensitive, being moderate (*rsw7*) or negligible (*rsw4*) at the permissive temperature, 19°C, and pronounced at the restrictive temperature, 30°C. After transfer to 30°C, the primary root's elongation rate decreases and diameter increases, with all tissues swelling radially. Swelling is accompanied by ectopic cell production but swelling is not reduced when the extra cell production is eliminated chemically. A double mutant was generated, whose roots swell constitutively and more than either parent. Based on analytical determination of acid-insoluble glucose, the amount of cellulose was normal in *rsw4* and slightly elevated in *rsw7*. The orientation of cortical microtubules was examined with immunofluorescence in whole mounts and in semi-thin plastic sections, and the orientation of microfibrils was examined with field-emission scanning electron microscopy and quantitative polarized-light microscopy. In the swollen regions of both mutants, cortical microtubules and cellulose microfibrils are neither depleted nor disoriented. Thus, oriented microtubules and microfibrils themselves are insufficient to limit radial expansion; to build a wall with high mechanical anisotropy, additional factors are required, supplied in part by RSW4 and RSW7.

Key words: *Arabidopsis thaliana*, Cell wall, Growth anisotropy, Microfibrils, Microtubules, Polarized-light microscopy

INTRODUCTION

The forms of plant organs are not only beautiful, they define plant performance. The ability of leaves to capture light optimally and of stems to give support, the ability of flowers to attract pollinators and of fruits to be dispersed, and the ability of roots to permeate the soil, all depend on the shape of the organ. A plant organ acquires a specific shape through control of growth. Plants control not only the overall rate of expansion, but also the rates of expansion in different directions. When growth rates in different directions are not equal, growth is said to be 'anisotropic'. Anisotropic growth varies both in the direction of maximal growth rate, as well as in the ratio of maximal to minimal growth rate (i.e., the degree of anisotropy). Growth anisotropy must be controlled to generate a plant organ with a specific form (Green, 1980).

The anisotropy of expansion is dictated by anisotropy in stress within a cell wall and in the wall's mechanical properties. The most prominent anisotropic component of the cell wall is cellulose. This polymer is synthesized at the plasma membrane as long chains of 1→4 β-linked glucose residues that associate laterally into microfibrils (Brown, 1999). Microfibrils are usually well oriented, which reinforces the cell wall anisotropically and guides the subsequent assembly of polymers around the cellulose framework (Cosgrove, 1997). Long-standing evidence shows that the ordered arrangement of microfibrils specifies the direction of maximal expansion (Green, 1980; Taiz, 1984). For example, in a rapidly elongating cell, the cellulose microfibrils are oriented on average perpendicular to the long axis of the cell and thus facilitate longitudinal expansion and hinder radial expansion. In turn, the orientation of microfibrils is commonly thought to be controlled in most cell types by the orientation of cortical microtubules (Baskin, 2001).

However, cellulose microfibrils themselves do not restrict expansion in the direction parallel to their long axes. This can

be appreciated by considering a cylindrical cell with transverse microfibril alignment and realizing that when the cell expands radially, the microfibrils themselves are not stretched, because they do not encircle the cell in closed loops. Instead, neighboring microfibrils slide past one another. Resistance to this shear limits radial expansion, a resistance presumably mediated by the matrix enmeshing the microfibrils. Efforts to understand how the cell wall matrix is remodeled to permit growth have focused exclusively on elongation (Cosgrove, 1997), and consequently we have very little idea whether elongation and radial expansion are governed by the same interactions between matrix and microfibrils.

As an approach to understand the control of anisotropic expansion, we are using developmental genetics, studying mutants in which this control is reduced or lost. We previously reported the isolation of mutants at three different loci, *RSW1*, *RSW2*, *RSW3*, that have swollen roots (called 'Rsw' for radially swollen) (Baskin et al., 1992), and others have isolated mutants with similar root swelling phenotypes (Benfey et al., 1993; Holding et al., 1994; Hauser et al., 1995; Scheres et al., 1995). Consistent with the central role of microtubules and microfibrils in determining growth anisotropy, these screens have identified loci required for the synthesis of cellulose or for the assembly of normal arrays of microtubules. *RSW1* (Arioli et al., 1998) and *PROCUSTE* (Fagard et al., 2000) encode catalytic subunits of cellulose synthase, *RSW2* (allelic to *KORRIGAN*) has been shown to encode an endo-1,4 β-glucanase that apparently functions in the synthesis of cellulose (Nicol et al., 1998; Lane et al., 2001; Sato et al., 2001), and *RSW3* encodes glucosidase II (J. Burn, personal communication), an ER enzyme in the N-glycosylation pathway whose operation is needed for cellulose synthesis. Other mutants that produce swollen roots have severely defective cortical microtubules: *tonneau1* and *ton2/fass* (Traas et al., 1995; McClinton and Sung, 1997), *botero/fragilefiber2* (Bichet et al., 2001; Burk et al., 2001) and *microtubule organization1* (Whittington et al., 2001).

We report here the characterization of mutants at two new loci, *RSW4* and *RSW7*. Despite the extensive root swelling of mutants at these loci, the orientations of cortical microtubules and of cellulose microfibrils closely resembled those of the wild type. These loci thus define novel activities controlling the anisotropic expansion of plant cells.

MATERIALS AND METHODS

Plant material and growth conditions

Seeds of *Arabidopsis thaliana* L. (Heynh) ecotype Columbia were mutagenized with ethane-methylsulfonate as described by Baskin et al. (Baskin et al., 1992), and lines used here were selfed for five generations and backcrossed at least once to wild type. Lines backcrossed 7 times have similar phenotypes. Seeds were sterilized in dilute bleach and germinated on nutrient-solidified agar supplemented with 3% sucrose in Petri plates, sealed with air-permeable bandage tape, and seedlings were grown vertically under continuous yellow light (80 μmol/m^{2}s) and constant temperature (19°C, permissive temperature) for up to 10 days in a growth chamber, as described by Baskin and Wilson (Baskin and Wilson, 1997). To cause expression of the swelling phenotypes, the plates were transferred to 30°C (non-permissive temperature) under continuous yellow light (50 μmol/m^{2}s) in a custom made growth chamber modified from a commercial 'frost-free' freezer, with light from 20 W cool-white and warm-white fluorescent tubes filtered through yellow acrylic (Plexiglas J2208, Cope Plastic, St. Louis, MO).

Elongation rate was measured by photographing seedlings on plates with a camera inside the chamber as described by Baskin et al. (Baskin et al., 1992), whereas root diameter was measured at the end of the treatment at the position of apparent maximal swelling or, if none, at the site of root hair initiation by means of a compound microscope and video digitizer. For experiments involving ethylene exposure, seeds were germinated on plates containing 100 μM $AgNO_3$. After 7 days wild-type seedlings were transferred to plates containing the same compound ±1 μM 1-aminocyclopropane-1-carboxylic acid (ACC; Sigma, St Louis, MO) and all treatments were transferred to 30°C for 2 days. For inhibitor experiments, seedlings were grown at 19°C for 6 days and then transplanted onto plates containing either 0.1% (v/v) DMSO (controls), 1 μM oryzalin (Chem Service, West Chester, PA), 1 μM 2, 6-dichlorobenzonitrile (DCB; Sigma), or 10 μg/ml aphidicolin (Sigma) and transferred to 30°C for 2 days. Stocks of oryzalin, ACC, DCB and aphidicolin were made in DMSO and stored at –20°C. An aqueous silver nitrate stock was made fresh for each experiment.

Genetic mapping

Genomic DNA was extracted from individual mutant F_2 plants from a cross to Landsberg *erecta*, cut with *Eco*RI, blotted, and probed with pooled probes (Fabri and Schäffner, 1994). Recombination percentages were obtained for 28-34 genomes, and converted to centiMorgans with the Kosambi function (Koornneef and Stam, 1992).

Measurement of tissue area and cell number

Seedlings were fixed and embedded in butyl-methyl methacrylate, as described by Baskin and Wilson (Baskin and Wilson, 1997). To measure tissue area, cross sections were collected every 10th μm spanning the region of maximal swelling (~200-500 μm from the tip), and four sections selected for measurement having the largest overall diameters. To count cells, cross sections were collected at 50 μm intervals within a region where swelling was extensive. Four roots were sectioned per treatment and five sections per root were scored. Sections were stained with periodic-acid-Schiff's (PAS), in a simplified procedure where sections were incubated in 1% periodic acid for 10 minutes, rinsed briefly in water, stained in Schiff's reagent (Sigma) for 30-60 minutes, and then rinsed extensively with water. We determined that roots did not shrink during processing by finding that the average diameter for wild-type roots freshly sectioned was 109±1.2 μm versus 111±5.3 μm for fixed, embedded and sectioned roots (mean ± s.e.m., n=4). Carlemalm et al. (Carlemalm et al., 1982) likewise reported no shrinkage for a similar mixture of methacrylates.

Localization of microtubules

For localizing microtubules in whole mounts of intact roots, seedlings were fixed, extracted in EGTA followed by pectinase, incubated in antibodies, and observed with confocal fluorescence microscopy, as described for *A. thaliana* by Liang et al. (Liang et al., 1996). For localizing cortical microtubules in sections, material embedded in methacrylate was processed for immunocytochemistry as described previously (Baskin and Wilson, 1997).

Analysis of monosaccharides

Seedlings were grown for 2 days at 21°C and then for 5 days at 30°C. As previously described (Lane et al., 2001), cell walls were collected from whole seedlings and incubated for 1 hour in 2 M trifluoroacetic acid at 120°C, and cellulose was determined as acid-insoluble glucan by gas chromatography and mass spectrometry; additionally, monosaccharides from non-cellulosic polysaccharides solubulized by acid were quantified.

Field-emission scanning electron microscopy (FESEM)

To image the innermost layer of the cell wall, intact seedlings were plasmolysed in 1 M sucrose for 45 minutes, fixed in 4% paraformaldehyde in 10 mM Pipes pH 7.0, and 0.5 M sucrose for 2 hours at room temperature, rinsed briefly in that buffer minus the fixative. Root tips were excised and sandwiched between Formvar films on wire loops as described by Baskin and Wilson (Baskin and Wilson, 1997). Root tips were infiltrated into polyethylene glycol (PEG) following a protocol modified from that of Fowke et al. (Fowke et al., 1999). Samples were first brought to 40% PEG 400 by stepwise exchange of the 0.5 M sucrose, and then to 100% PEG 400. Samples were then placed at 55°C and progressively infiltrated first with PEG 1000, then with a 3:1 (v/v) mixture of PEG 1450:PEG 1000 over the following 2 days, and then embedded. After excising the wire loop from the block, nominally 15 μm thick sections were cut at 16°C and collected on coverslips previously sputter-coated with approximately 20 nm of gold or gold-palladium followed by brief incubation in 0.1% (v/v) polyethylene-imine. The metal reduced charging and the imine adhered the sections. The coverslips with sections were warmed on a slide warmer for 30 minutes at 40°C to flatten the sections and they were stored in a desiccated state. Coverslips were immersed in distilled water to remove the embedment, incubated in 30 μg/ml proteinase K for 1 hour then in a solution of 250 mM NaCl and 0.05% (v/v) Triton X-100 for 3 hours or overnight to remove adherent cytoplasts, rinsed three times briefly in distilled water, dehydrated to 100% ethanol, critical point dried, and sputter coated with a thin film of platinum (nominally 2 nm).

As an alternative to PEG embedment, some samples were prepared using the protocol developed by Sugimoto et al. (Sugimoto et al., 2000) in which roots were cut open with a cryo-ultramicrotome, cytoplasm was removed with bleach, and samples then dehydrated, critical point dried, and sputter-coated with platinum. Samples prepared by either method were examined with a FESEM (Hitachi 4500 or Hitachi 4700S). For quantification of microfibril angles, cells were selected at low magnification where microfibrils were invisible and then an image captured at a magnification of 60,000 times. A region of interest (256×256 pixels) was selected and the 2D Fourier transform calculated (Image Processing Toolkit, version 3, Reindeer Games, Chapel Hill NC). The transforms were elliptical and the angle was measured between the major axis of the ellipse and the transverse (defined as 0°), an angle that estimates the net orientation of microfibrils.

Polarized-light microscopy

Methacrylate sections (2 μm thick) were mounted in 75% glycerol, 0.1% Triton X-100 and examined through a polarizing microscope (Jenapol, Carl Zeiss Jena). Birefringent retardation was assessed in longitudinal cell walls that were parallel to the section plane, and was quantified with microphotometry. The light intensity passing through a square aperture, placed first over a cell wall and then over the background, was measured at ±45° settings of a compensator (Brace-Köhler type, Γ_{max}=18 nm) and retardation was calculated from the intensity measurements, as described by Baskin et al. (Baskin et al., 1999). The area of the selected cell wall was always larger than the area sampled by the aperture (3.75 μm^2) and the aperture was placed near the center of the selected cell wall, thus minimizing aberrations due to the presence of edges. The aperture was also placed to avoid any visible heterogeneity in the cell wall, such as that caused by pit fields.

RESULTS

RSW4 and *RSW7* define new loci

The mutants, *rsw4* and *rsw7*, were isolated on the basis of a temperature-dependent stimulation of radial swelling in the primary root (Fig. 1A-C). The F_1 progeny of back-crosses to wild type were exposed to 30°C for 2 days and scored for root swelling. None of the F_1 seedlings had swollen roots, and in the F_2, wild-type and mutant phenotypes segregated indistinguishably from a 3:1 ratio (Table 1), indicating the recessive, monogenic nature of the mutations. Analysis of restriction fragment polymorphism mapped *RSW4* to the lower arm of chromosome IV (12±5.9 cM from m326B, map position 61.9) and *RSW7* to the lower arm of chromosome II (3.1±3.1 cM from m283C, map position 61; and 13±6.2 cM from m336a, map position 78.4).

To ascertain allelic relationships, pairwise crosses were

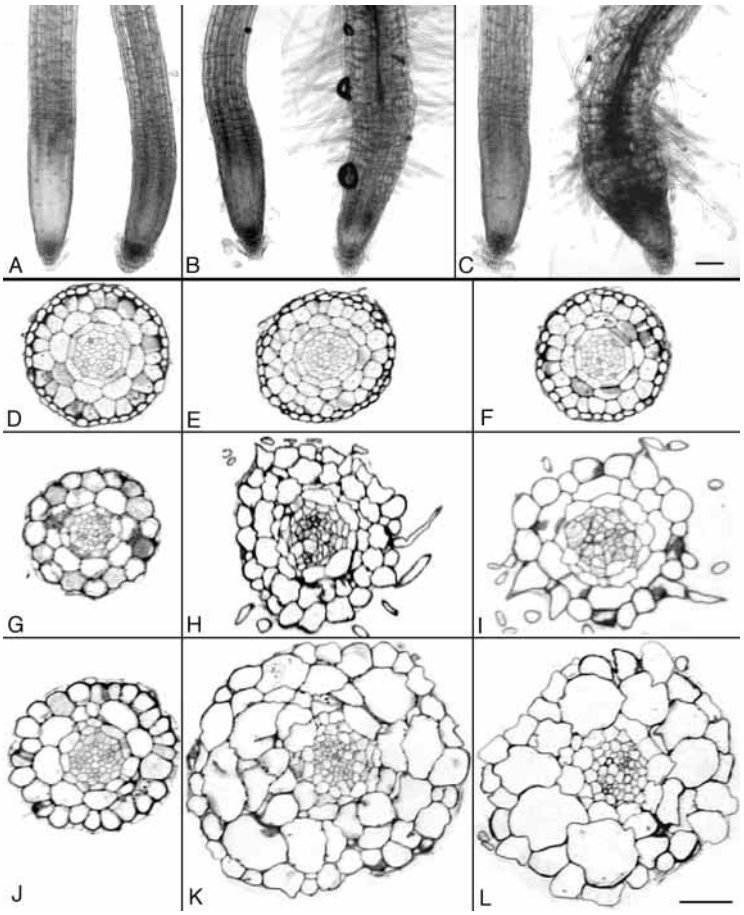

Fig. 1. Light micrographs showing morphology and histology of *rsw4* and *rsw7* roots. (A-C) Paired images of a roots grown under (left-hand image) the permissive treatment (8 days at 19°C) and under (right-hand image) the restrictive treatment (6 days at 19°C followed by 2 days at 30°C). (A) Wild type; (B) *rsw4*; (C) *rsw7*. Bar: 100 μm. (D-L) Cross sections of roots within the region of maximal diameter stained with PAS to show cell walls: (D-F) Wild type; (G-I) *rsw4*; (J-L) *rsw7*. The left hand column (D,G,J) shows the anatomy of plants grown under the permissive treatment, the center column (E,H,K) the restrictive treatment, and the right-hand column (F,I,L) the permissive treatment supplemented with 10 μg/ml aphidicolin for the 2 days at 30°C (wt and *rsw7*) or for only the second day (*rsw4*). Bar: 50 μm.

Table 1. F_2 segregation data of *rsw4* and *rsw7* back crossed to wild type

	Wild type			Mutant		
Genotype	*n**	Obs†	Exp‡	Obs†	Exp‡	χ^2
rsw4	396	303	297	93	99	0.48
rsw7	372	288	279	84	93	1.16

*Total number of seedlings observed.

†Number of seedlings observed with either the wild-type or mutant phenotype.

‡Number of seedlings expected from a back cross of a homozygous recessive mutant to wild type with a segregation ratio of 3:1.

None of the observed frequencies differed significantly from those expected for a recessive allele at a single locus. A departure from the expected frequency significant at the 95% level would yield a χ^2 value of 3.84.

made between the mutants and other known radial swelling mutants: *rsw1*, *rsw2*, *rsw3* (Baskin et al., 1992), *rsw5*, *rsw6* and *rsw8* (Wiedemeier, 1998). All of these crosses produced phenotypically wild-type F_1 offspring, indicating complementation. *RSW4* maps near *CUDGEL*, and *RSW7* maps near *POMPOM2* and *MOR1*, loci previously identified as being involved in root morphology (Hauser et al., 1995; Whittington et al., 2001). As the only known mutant *cud* allele is fully dominant and gametophytic lethal, complementation could not be tested; however, crosses between *rsw7* and *pom2*, as well as between *rsw7* and *mor1*, produced progeny with only a wild-type phenotype. On this basis, *RSW4* and *RSW7* are defined as new loci.

From the cross between *rsw4* and *rsw7*, we isolated a putative double mutant. When this line was back crossed to each parent, all progeny were mutant, confirming the double mutant genotype. The radial swelling phenotype of the double mutant was expressed constitutively, and was more extreme than either parent (data not shown). Thus, RSW4 and RSW7 represent two different and additive activities needed to control the anisotropic expansion of the root.

Growth anisotropy and cell wall placement

When grown at the permissive temperature (19°C), the mutants resembled wild type, but when transferred to the restrictive temperature (30°C), the roots became swollen (Fig. 1A-C). At 19°C, *rsw4* roots elongated slightly more slowly and *rsw7* roots considerably more slowly than wild-type roots (Fig. 2A), and *rsw4* root diameter was the same as wild type but *rsw7* was somewhat greater. With transfer to 30°C, root elongation in all three genotypes was transiently stimulated and then inhibited (Fig. 2B), a pattern previously reported for the wild type and other Rsw mutants (Baskin et al., 1992). The roots of *rsw4* and *rsw7* elongated similarly, and after 24 hours attained a low but non-zero rate. In contrast, they differed in radial expansion: *rsw7* responded sooner and reached a greater maximum than *rsw4* (Fig. 2C). In the wild type, cells expand radially at negligible rates, resulting in the root's growth zone being strictly cylindrical; therefore, the stimulated radial expansion in the mutants indicates that the degree of growth anisotropy was reduced.

We examined root anatomy to determine whether radial expansion was accompanied by ectopic cell production or was confined to specific tissues. Seedlings were transferred to the

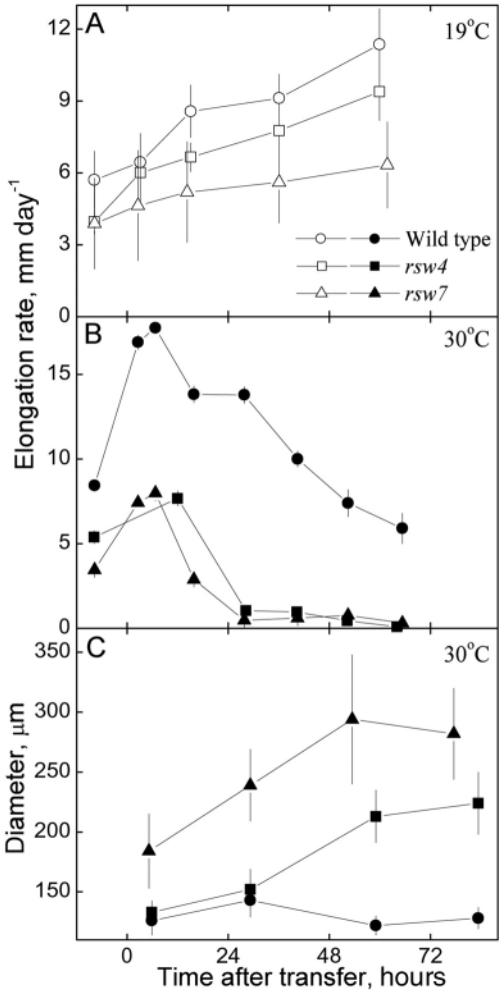

Fig. 2. Growth kinetics of *rsw4* and *rsw7* roots. Seedlings were transferred to 30°C (time zero on the *x*-axis) after 6 days at 19°C. (A,B) Elongation rate; (A) mean±s.d. of 10 seedlings or (B) mean±s.e.m. of 3-6 plates. (C) Root diameter; mean±s.d. of 10 seedlings.

restrictive temperature for 2 days, and then fixed, embedded and cross-sectioned. At 19°C, the mutants resembled wild type, although *rsw7* had extra cells, whereas at 30°C, both mutants formed extra cells with cell walls at unusual positions and orientations, tending to obscure tissue boundaries (Fig. 1). We defined the outer tier of cells as the epidermis, the inner group of small cells as the stele, and estimated the boundary between cortex and endodermis based on cell shape. Compared to wild type, the area of tissues in the mutants was slightly greater at 19°C and more than double at 30°C (Fig. 3), showing that all tissues were affected. Likewise, cell numbers tended to increase in all tissues (Table 2). Except for epidermis in *rsw7*, in which cell number increased slightly, the 2 days incubation at 30°C increased cell number in both mutants by approximately 1.3 fold.

To determine if the ectopic cells divisions were necessary for the reduced growth anisotropy, seedlings were transferred to plates containing the cell division inhibitor, aphidicolin, at 10 µg/ml, a concentration that we have found reduces proliferative divisions in the wild type by more than 50% (data not shown). At 30°C, aphidicolin blocked the increase in cell

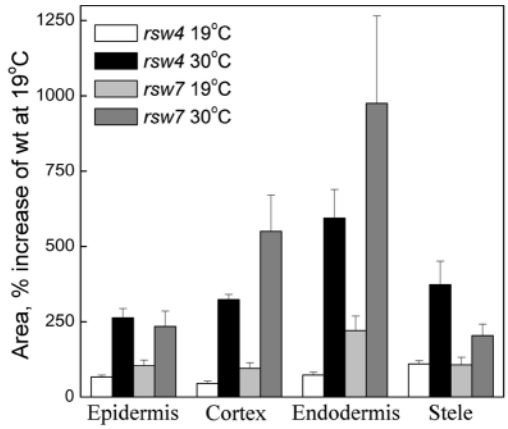

Fig. 3. Tissue areas of *rsw4* and *rsw7* roots. Area per tissue for *rsw4* at 19°C (white bars), *rsw4* at 30°C (black bars), *rsw7* at 19°C (light-gray bars) and *rsw7* at 30°C (dark-gray bars) expressed as the percent increase of the area in wild type grown at 19°C. All treatments were for 8 days, with 30°C for the final 2 days. Data are means±s.e.m. of 4 roots with 4 sections per root.

number almost totally but scarcely reduced root swelling (Fig. 1; Table 2). Similarly, in experiments without aphidicolin, we cut sections from roots fixed 2 hours after increased radial expansion first became detectable and found no significant increase in cell numbers (data not shown). Therefore, defective cell division is unlikely to explain the root swelling and an explanation must be sought in the process of expansion.

Role of ethylene, microtubules and microfibrils in root swelling

Because the directionality of cell expansion is known to be influenced by ethylene and because ethylene causes the production of ectopic root hairs, as does *rsw4* (Fig. 1H,I), seedlings were grown for 7 days on 100 μM silver nitrate, which is an inhibitor of ethylene action (Beyer, 1976), and then transferred to 30°C for 2 days. Silver nitrate completely suppressed the swelling of wild-type seedlings treated with an ethylene precursor (1 μM ACC), but had no significant effect on the swelling of either mutant (data not shown). Therefore, swelling in *rsw4* and *rsw7* is not stimulated by ethylene.

To examine the role of microtubules and cellulose microfibrils in the phenotypes of the mutants, we exposed them at 30°C either to 1 μM oryzalin, which depolymerizes nearly all microtubules from *A. thaliana* roots (Baskin et al., 1994), or to 1 μM DCB, which inhibits cellulose synthesis (Hogetsu et al., 1974). At 30°C, root diameter of both mutants on oryzalin or DCB was significantly increased (Table 3). By contrast, root diameter of another temperature-sensitive radially swollen mutant, *rsw1*, was not significantly increased by DCB, but was by oryzalin (Table 3). Because *rsw1* has low rates of cellulose synthesis (Arioli et al., 1998; Peng et al., 2000), DCB may be unable to increase root swelling further. Conversely, because root swelling in *rsw4* and *rsw7* was increased by oryzalin or DCB, this suggests that both mutants had microtubules and microfibrils that remained, at least partially, functional.

Cortical microtubule orientation in the growth zones of *rsw4* and *rsw7*

The cortical microtubule arrays of each mutant were examined using indirect immunofluorescence with confocal microscopy for intact roots and with conventional epifluorescence for semi-thin sections of roots embedded in butyl-methyl-methacrylate. The confocal preparations allowed the microtubule arrays to be viewed in three dimensions, but only in epidermal cells; whereas, in the sections it was possible to view the microtubules in all tissues but only in glancing sections through the cell cortex. Both the epidermis, viewed with confocal optics (Fig. 4A-C), and all tissues viewed in the sections (Fig. 4D-F) had abundant cortical microtubules within growing regions that were oriented predominantly transverse to the root's long axis. It appears that swelling in *rsw4* or *rsw7* was not accompanied by any marked depletion or disorientation of cortical microtubules.

Cellulose microfibrils in the growth zones of *rsw4* and *rsw7*

To examine cell wall synthesis in these mutants, we analyzed the levels of monosaccharides. Newly germinated seedlings were transferred to the restrictive temperature and grown for 5 days to enrich for cell wall formed at 30°C. The cell walls were then hydrolyzed with trifluoro-acetic acid to yield soluble and insoluble (i.e., cellulose) fractions. Compared to wild type, cellulosic glucose was not changed significantly in *rsw4* whereas it was raised by about 13% in *rsw7* (Fig. 5). This pattern differs from prominent decreases in cellulosic glucose previously reported in root swelling mutants (Peng et al., 2000; Schindelman et al., 2001).

Additionally, we quantified monosaccharides present in the soluble fraction. Rhamnose was not affected; fucose decreased in *rsw4* to a small, marginally significant extent; and the other sugars increased, with *rsw4* having consistently larger increases than *rsw7* (Fig. 5). The pattern of sugars does not implicate a specific class of cell wall polymer but instead suggests a global defect in cell wall metabolism.

Table 2. Root diameter and cell number in *rsw4* and *rsw7* at permissive and restrictive temperatures and in the presence or absence of aphidicolin (10 μg/ml)

	Cell number in epidermis			Cell number in rest of root			Root diameter (μm)		
Treatment	wt	*rsw4*	*rsw7*	wt	*rsw4*	*rsw7*	wt	*rsw4*	*rsw7*
19°C+0.1% DMSO	23.4±0.3	17.7±0.5	25±1.4	63.8±1.3	63.9±1.9	85.6±6	186±3	198±2	246±7
30°C+0.1% DMSO	24.7±1	23.3±1.7	26.7±1.1	62.3±3.3	82.5±4.2	111±4.4	166±4	255±7	357±9
30°C+aphidicolin	23.7±1.5	20.7±0.8	26.7±0.8	59.7±4.6	68.7±1.6	85.6±2.1	164±1	256±6	318±12

Data for root diameter are means±s.e.m. of three plates; data for cell number were counted from cross-sections and are means±s.e.m. of four roots, each with 5 sections collected at 50 μm intervals through the region of maximal swelling. Seedlings were grown for 6 days at 19°C, transplanted onto control (DMSO) or aphidicolin plates, and grown for a further 2 days at 30°C (*rsw4* was transplanted on the second day at 30°C).

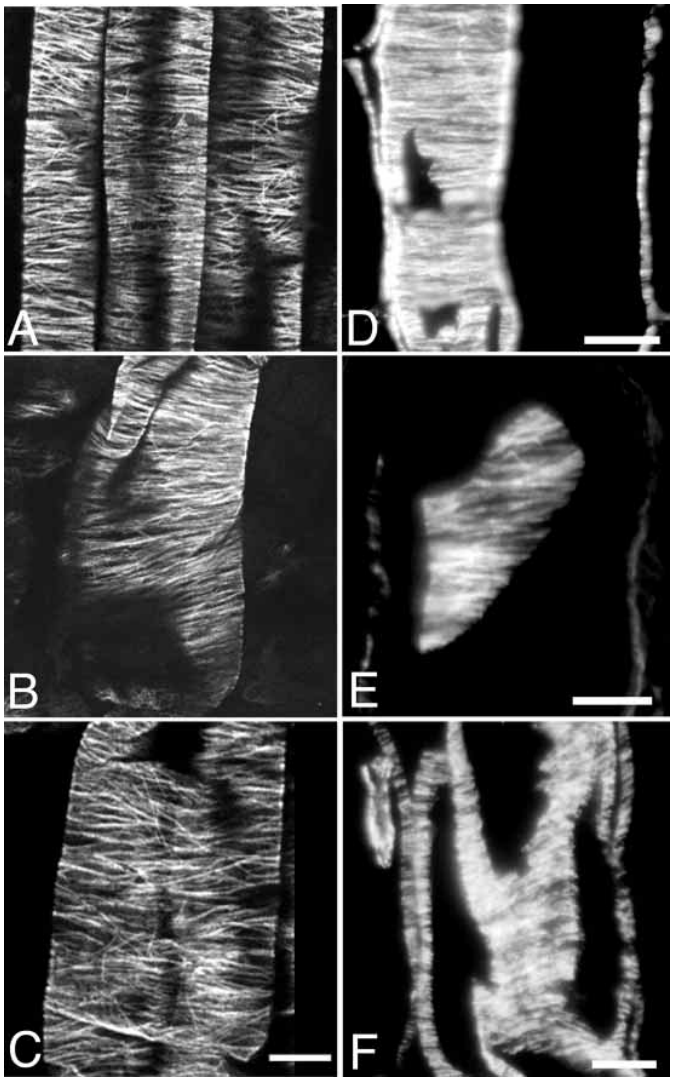

Fig. 4. Cortical microtubules of wild type, *rsw4* and *rsw7* in the elongation zone (wild type) or swollen region of the root. (A-C) Cortical microtubules in epidermal cells imaged with confocal microscopy. (D-F) Cortical microtubules in root cortex imaged in longitudinal methacrylate sections. (A,D) Wild type, (B,E) *rsw4* and (C,F) *rsw7* plants grown at 19°C for 6 days and transferred to 30°C for 2 days. Bars: 10 μm.

Table 3. Root diameters of wild type and 3 Rsw mutants treated with the microtubule inhibitor, oryzalin, or the cellulose synthesis inhibitor, 2,6-dichlorobenzonitrile (DCB)

	Diameter (μm)		
Genotype	30°C+0.1% DMSO	30°C+1 μM oryzalin	30°C+1 μM DCB
Wild type	128±5	455±9	371±11
rsw1	342±6	411±11	333±13
rsw4	186±5	407±4	393±5
rsw7	236±16	427±10	414±4

Data are means±s.e.m. from 3-4 replicate experiments, with one plate of 10 seedlings per experiment. Seedlings were grown for 6 days at 19°C, transplanted onto control (DMSO) or inhibitor plates, and grown for a further 2 days at 30°C. Absolute values for diameter in this experiment differ from those in the experiment in Table 2 for unknown reasons.

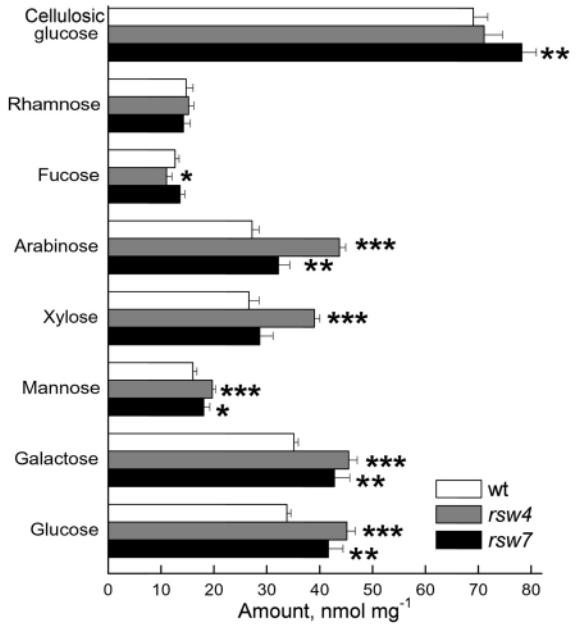

Fig. 5. Analysis of monosaccharides in wild type, *rsw4*, and *rsw7* cell walls. The levels are expressed per mg of cell wall dry weight. Cellulosic glucose is the material that is insoluble in boiling trifluoroacetic acid. Data are mean of 4 replicate determinations±s.d. Significance was tested with two-tailed, paired *t*-tests, mutant versus wild type, and indicated when equivalence of means was rejected by **P*<0.05, ***P*<0.01 or ****P*<0.001.

In addition to cellulose synthesis, we assayed cellulose microfibril orientation, imaging microfibrils at the innermost layer of the cell wall with FESEM. Seedlings were plasmolysed, fixed and embedded in PEG, and then sectioned. Plasmolysis separates the membrane from the cell wall, which otherwise sticks tightly, and PEG is removable after sectioning with water, thus exposing the surface of the cell wall for imaging without harsh extraction. In wild-type roots, in the elongation zone, microfibrils were dense, well aligned, and had a predominantly transverse orientation (Fig. 6A). Likewise, in swelling regions of the mutants, microfibrils appeared densely aligned and had a transverse orientation (Fig. 6B,C). For *rsw4*, we quantified the net orientation of microfibrils in cells chosen at random within the first 400 μm from the tip and found that the net alignment was not significantly different from transverse (2.0±3.5°, transverse=0°; mean±s.e.m., *n*=5; 12-24 cells per section). However, for *rsw7*, it was impossible to examine enough cells for quantification because the roots often fragmented in sectioning and many cell walls appeared to remain covered by the plasma membrane.

To confirm the results with FESEM, we used polarized-light microscopy, a technique that is quantitative and allows many cell walls to be measured. Roots were embedded in methacrylate and sectioned longitudinally, and cell walls within the plane of the section were examined. In the elongation zone of the wild type, cell walls had an extinction angle that was perpendicular to the long axis of the root, and interacted with the compensator as expected for transverse microfibrils (Fig. 7A,B) (Preston, 1974). Similarly, in both mutants, although the cell walls were present in the plane of the section only in scattered irregular areas, they did behave

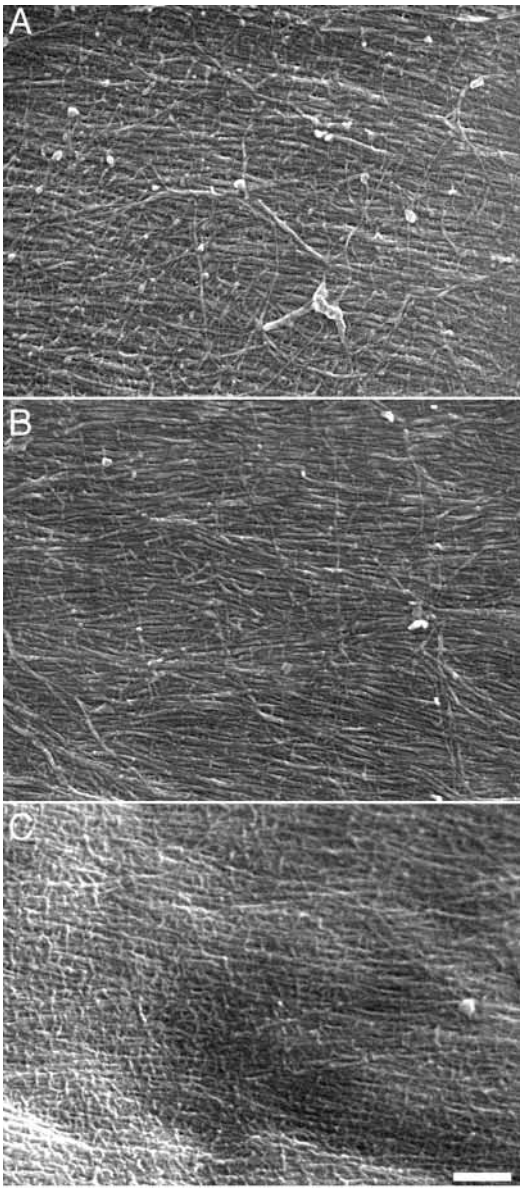

Fig. 6. FESEM micrographs of the innermost cell wall layer of wild type, *rsw4* and *rsw7* plants in the elongation zone (wild type) or swollen region of the root. (A-C) Longitudinal-radial cell walls with the long axis of root parallel to the long axis of the page. (A) Wild type, (B) *rsw4* and (C) *rsw7*, grown at 19°C for 6 days and transferred to 30°C for 2 days. (A-B) PEG sections, (C) cryo-ultramicrome. Bar: 100 nm.

comparably to those of the wild type in polarized light (Fig. 7C-F). This indicates that both mutants, like the wild type, had microfibrils with a net transverse alignment.

To examine the degree of orientation of the microfibrils, we quantified the birefringent retardation of cell walls using microphotometry. In the wild type, retardation remained roughly constant through the first 600 μm of the root, and was not affected by a 2 days exposure to the non-permissive temperature (Fig. 8A). In wild-type roots treated for 12 hours with DCB, or in *rsw1* roots exposed to 30°C for 12 hours, retardation decreased significantly (Fig. 8B), as expected when cellulose synthesis is inhibited. In contrast, the retardation of cell walls of both *rsw4* and *rsw7* was not less than the wild type, and in fact, tended to be greater (Fig. 8C,D). In *rsw4*, at 19°C, despite having wild-type levels of radial expansion (i.e., normal morphology), roots had somewhat higher levels of retardation in their cell walls, and at 30°C, despite the stimulated radial expansion, retardation in the walls remained essentially unchanged. In *rsw7*, increased radial expansion at 30°C was associated with a clear increase in retardation, especially in the apical 200 μm. Decreases in retardation were not seen in these mutants, which indicates that the degree of orientation among cellulose microfibrils did not decrease.

Taking the sugar analysis together with the FESEM images and the polarized-light data, we conclude that both mutants had reduced growth anisotropy without a decline in cellulose synthesis or a disorientation among cellulose microfibrils.

DISCUSSION

We investigated the underlying causes of the reduced growth anisotropy of two mutants of *Arabidopsis thaliana*, *rsw4* and *rsw7*. Anisotropic expansion is currently understood to be controlled by the orientation of cortical microtubules and cellulose microfibrils and we focussed on these elements. The orientation of cortical microtubules was not conspicuously altered nor was their abundance reduced appreciably; likewise, cellulose synthesis was not reduced nor were microfibrils disoriented. To our knowledge, the results here are the first demonstration of disrupted morphogenesis in the diffuse growing cells of higher plants without a concomitant disruption of the orientation of either cortical microtubules or cellulose microfibrils.

One consequence of both the *rsw4* and *rsw7* mutations is the disruption of the normal pattern of cell wall placement, which may include a breakdown of tissue boundaries. A similar disruption of the orientation of cell division occurs in some other *A. thaliana* mutants with reduced growth anisotropy, including *kor* (Lane et al., 2001) and *fra2* (Burk et al., 2001), but not in others, such as *cobra* (Schindelman et al., 2001) or *rsw1* (Williamson et al., 2001). Disoriented planes of cell division in the mutants indicate that the specification of polarity in the root has been disturbed or that there are activities common to the control of the placement of the cell plate and cell wall extensibility.

Orientations of microtubules and microfibrils

We examined microtubules by two methods and both consistently showed transverse microtubules in regions of the mutant roots that were undergoing stimulated radial expansion. Microtubules beneath the outer epidermal cell wall when viewed with confocal optics were observed readily, but those in interior tissues examined in plastic sections were difficult to observe because of the irregular orientation of cell walls. It is unlikely that a cryptic disorganization among cortical arrays in the interior tissues causes the swelling. First, it is reasonable to expect radial swelling to have a common cause in all tissues. Second, aberrant microtubule behavior frequently gives rise to helical growth in roots, as seen with low concentrations of microtubule inhibitors (Furutani et al., 2000) and in plants mutant for α-tubulin, as described recently (Thitamadee et al.,

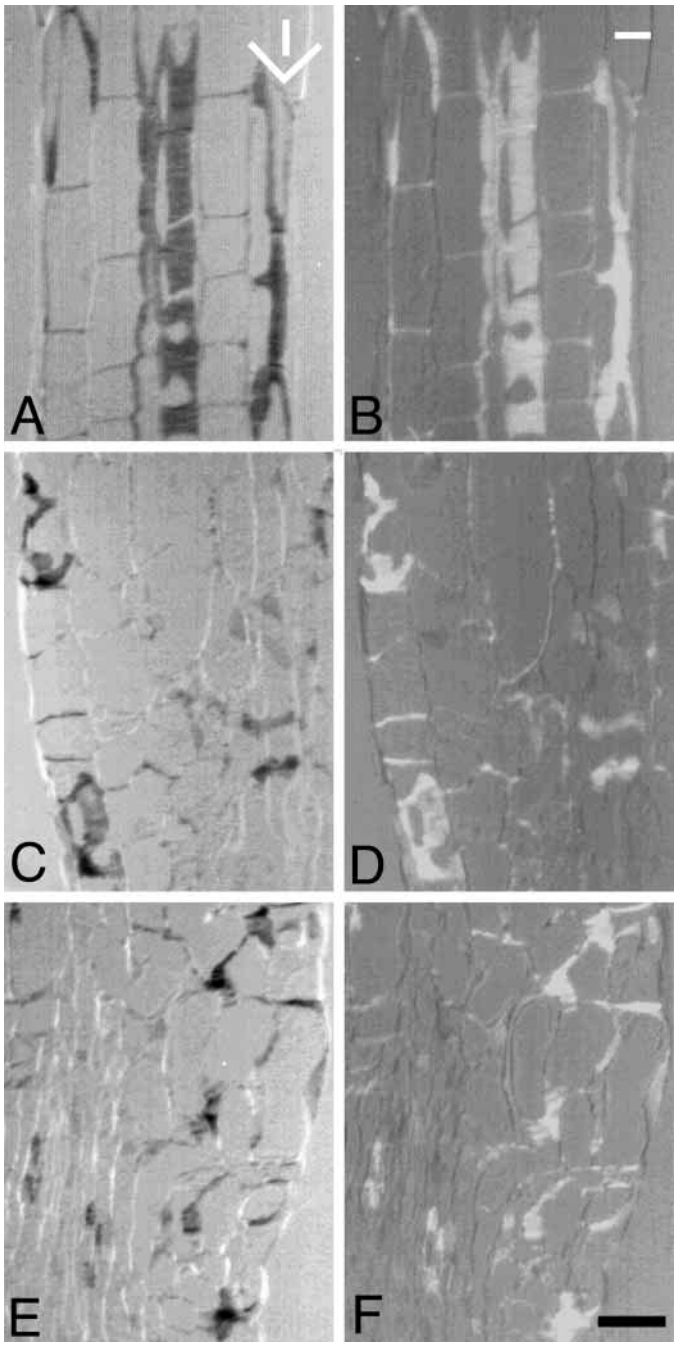

Fig. 7. Polarized-light micrographs of longitudinal sections of the elongation zone (in the wild type) or swollen region of the root in *rsw4* and *rsw7*. The transmission axes of analyzer and polarizer are shown by the white right-angle in (A). (A,C,E) The compensator was rotated to a positive angle, and (B,D,F) to a negative angle; the orientation of the white line in the two upper panels (A,B) shows the direction of the optical axis of birefringent elements (i.e., microfibrils) that would produce regions of the image brighter than background. (A,B) A section from wild type, (C,D) *rsw4* and (E,F) *rsw7* shown with each compensator setting. Seedlings were grown as for Fig. 4. The left-hand and right-hand panels were photographed with identical microscope settings and processed identically for reproduction. Bar: 25 μm.

2002); however, *rsw4* and *rsw7* seldom if ever grew helically, consistent with their having unimpaired microtubules. Finally, mutant alleles of genes encoding microtubule interacting proteins, including MOR1 (Whittington et al., 2001) and a katanin subunit (Bichet et al., 2001; Burke et al., 2001) cause radial swelling and disrupt microtubules unmistakably. Lack of obvious microtubule abnormalities in the *rsw4* and *rsw7* mutants predicts that the RSW4 and 7 proteins are unlikely to control cortical microtubule orientation.

Misalignment of microtubules alone might be insufficient to alter growth anisotropy: in wild-type *A. thaliana*, the cortical array can be disrupted considerably without reducing growth anisotropy (Baskin et al., 1994). Thus, we cannot exclude the possibility that a property of the microtubules other than orientation, such as their stability, could be altered in the *rsw4* and *rsw7* mutants, but it is not known how this would affect the anisotropy of expansion.

We assayed cellulose microfibrils in the growth zone with two complementary methods and both showed transverse orientation in the mutants. The use of polarized-light microscopy to quantify microfibril alignment is frequently criticized because the data apply to microfibrils throughout the thickness of the cell wall whereas load is said to be borne by the inner layers only (Taiz, 1984). However, in this study we show that birefringent retardation is significantly diminished in *rsw1* and in wild-type seedlings treated with DCB (Fig. 7), treatments known to reduce the rate of cellulose synthesis (Arioli et al., 1998; Peng et al., 2000) and disorganize recently deposited microfibrils (Sugimoto et al., 2001). Polarized-light microscopy thus has the required sensitivity for quantifying the deployment of cellulose microfibrils.

In contrast to the decreased retardation expected from the swollen morphology, and seen when cellulose synthesis was inhibited, retardation was unchanged in *rsw4* and actually increased in *rsw7* (Fig. 7). Increased retardation indicates better alignment among microfibrils or a greater quantity of microfibrils per unit of wall area. The quantity of microfibrils per unit area could increase through an increased rate of cellulose synthesis or a decreased rate of microfibril removal. As microfibrils are ‘removed’ principally by dilution through expansion and as the rate of expansion of the mutants was low, increased retardation probably occurred because expansion rate was inhibited. Consistently, more glucose was recovered from the acid-insoluble fraction of *rsw7* cell walls, indicating an increased quantity of cellulose. These results demonstrate that a major reduction in growth anisotropy can occur without lessening the overall structural anisotropy of the cell wall provided by oriented cellulose microfibrils.

To examine microfibril orientation directly, we used FESEM. To minimize the potential for rearrangement of microfibrils, we developed a protocol expected to extract components of the cell wall minimally, a protocol based on embedding plasmolysed roots in polyethylene glycol and subsequently removing the glycol embedment with water. This protocol succeeded for wild type and *rsw4*; however, *rsw7* roots were fragmented by the sectioning, suggesting that their middle lamellae may be weak. Furthermore, most cells of the *rsw7* root were not plasmolysed in 1 M sucrose, a resistance that implicates either an increased cellular osmolarity or an enhanced adhesion between the cell wall and the plasma membrane. To image the cell wall in *rsw7*,

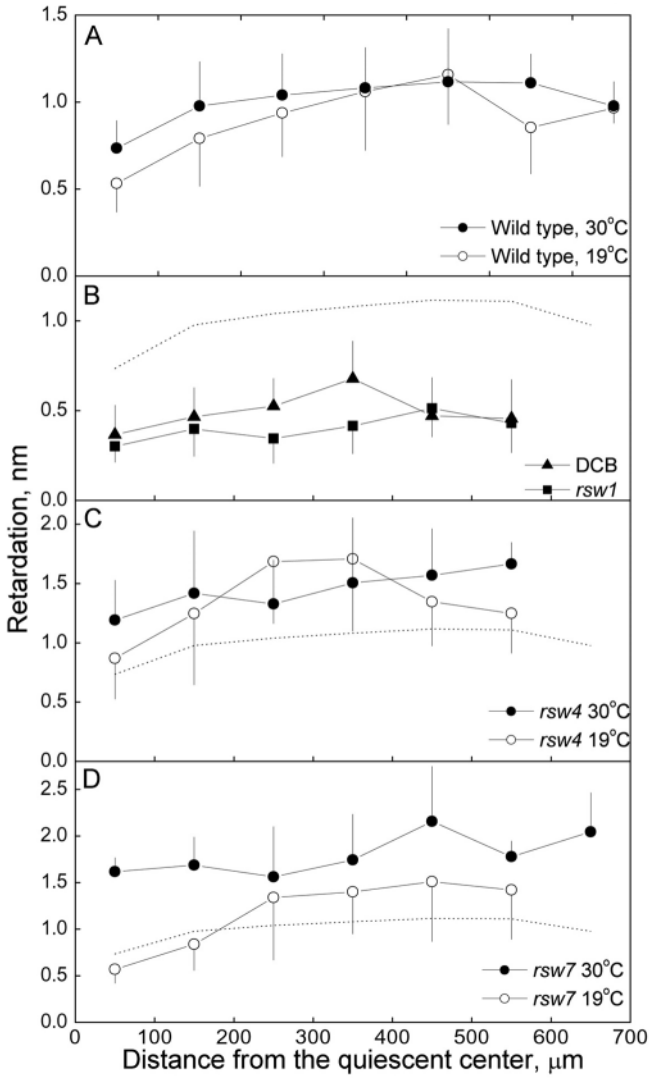

Fig. 8. Birefringent retardation versus distance from the quiescent center in cell walls of wild-type and mutant roots. (A,B) Wild type; (C) *rsw4*; (D) *rsw7*. (A,C,D) Data for seedlings grown for 8 days at 19°C (open circles), and seedlings grown for 6 days at 19°C and transferred to 30°C for 2 days (filled circles). (B) 8-day wild-type roots treated with 1 μM DCB for 12 hours at 30°C (filled triangles), and 8-day *rsw1* roots exposed to 30°C for 12 hours (filled squares). (B,C,D) The dotted line indicates the wild-type 30°C data from A. For each treatment, three sections from four roots were sampled, and symbols are means±s.d. of six to 21 cell walls located within 50 μm of the *x*-axis value.

we turned to a method developed recently by Sugimoto et al. (Sugimoto et al., 2000) in which the cells of the *A. thaliana* root are cut open by means of a cryo-ultramicrotome. The FESEM analysis confirmed the results from polarized-light microscopy, and taking both methods together, we conclude that *rsw4* and *rsw7* have a reduced degree of growth anisotropy despite having within their growth zones appropriately oriented, transverse microfibrils.

Control of anisotropic expansion

The control of plant shape has focused on the orientation of cellulose microfibrils (Green, 1980). The presence of aligned cellulose has long been considered necessary for anisotropic expansion, and reorientation of mean microfibrillar angle changes the direction of maximal expansion rate (Green, 1980; Taiz, 1984). The results here suggest that correctly oriented microfibrils, although necessary, are not sufficient to control growth anisotropy.

There are a few examples in the literature in which the alignment of microfibrils can be seen to be insufficient to specify the degree of growth anisotropy. First, the primary root of maize can change the degree of growth anisotropy independently of the orientation of cortical microtubules and cellulose microfibrils (Baskin et al., 1999). In this system, the spatial profile of growth anisotropy was found to vary appreciably during development, as well as when the roots were exposed to water stress, but the orientations of both microtubules and microfibrils throughout nearly the entire growth zone remained transverse. Baskin et al. (Baskin et al., 1999) hypothesized that expansion rates in length and in radius are regulated through the independent adjustment of the cell wall yielding in each direction. Consistent with this hypothesis, a pair of loci have been identified that exert independent control over growth in length and width of *A. thaliana* leaves (Tsuge et al., 1996).

Second, in the cladophoralean green alga, *Chaetomorpha moniligera*, growth became nearly isotropic when the diffuse-growing, cylindrical cells were exposed to colchicine, but electron microscopy of replicas showed that the deposition of alternating lamellae of longitudinal and transverse microfibrils was not affected (Okuda and Mizuta, 1987). Although these authors did not measure net orientation of microfibrils with polarized light and thus could not rule out a change in the relative thickness of longitudinal versus transverse lamellae, they did find evidence of aberrant secretion of cell wall matrix components, which may explain the loss of control over expansion anisotropy.

Finally, it has been recently shown that microfibril orientation is not disrupted in the roots of the *A. thaliana* mutant *mor1*, despite reduced growth anisotropy (Sugimoto, 2000). In *mor1*, cortical microtubules are disorganized, which suggests that microtubules may influence anisotropy by a mechanism other than through controlling the alignment of microfibrils. This mechanism plausibly involves targeted secretion, given the evidence from *C. moniligera* cited above and the involvement of microtubules in vesicle traffic. Intriguingly, the relevant components delivered by the microtubules might be missing or defective in *rsw4* and *rsw7*.

We hypothesize here that RSW4 and RSW7 influence the anisotropy of expansion by governing how well parallel microfibrils resist shear. As noted previously, models of cell expansion mainly address expansion perpendicular to the direction of microfibrils (that is, elongation) leaving few ideas of whether radial expansion is governed by similar factors. Interaction between microfibrils, whether by direct contact or by hemicellulose tethers, seems likely to be critical in the resistance offered to radial expansion. Knowing how RSW4 and RSW7 act should enrich models of cell wall architecture and deepen understanding of how higher plants control the anisotropic expansion of their cells and organs.

We thank Amy Gernstetter (UM), Rosemary Birch (ANU) and Ann Cork (ANU) for technical help; Dr Jane Murfett (UM) for assistance

with RFLP mapping, the Electron Microscopy Unit (ANU) and the Core Facility for Electron Microscopy (UM) for help with electron microscopy, and Keiko Sugimoto (ANU) for help with cryo-ultramicrotomy and insightful discussions about FESEM. A. M. D. W. was supported by a Patricia Roberts Harris Fellowship. This project was funded in part by a grant to T. I. B. from the US Department of Energy (award No. 94ER20146), which does not constitute endorsement by that Department of views expressed herein.

REFERENCES

Arioli, T., Peng, L., Betzner, A. S., Burn, J., Wittke, W., Herth, W., Camilleri, C., Höfte, H., Plazinski, J., Birch, R. et al. (1998). Molecular analysis of cellulose biosynthesis in Arabidopsis. *Science* **279**, 717-720.

Baskin, T. I. (2001). On the alignment of cellulose microfibrils by cortical microtubules: a review and a model. *Protoplasma* **215**, 150-171.

Baskin, T. I. and Wilson, J. E. (1997). Inhibitors of protein kinases and phosphatases alter root morphology and disorganize cortical microtubules. *Plant Physiol.* **113**, 493-502.

Baskin, T. I., Betzner, A. S., Hoggart, R., Cork, A. and Williamson, R. E. (1992). Root morphology mutants in *Arabidopsis thaliana*. *Aust. J. Plant Physiol.* **19**, 427-437.

Baskin, T. I., Meekes, H. H. T. M., Liang, B. M. and Sharp, R. E. (1999). Regulation of growth anisotropy in well watered and water-stressed maize roots. II. Role of cortical microtubules and cellulose microfibrils. *Plant Physiol.* **119**, 681-692.

Baskin, T. I., Wilson, J. E., Cork, A. and Williamson, R. E. (1994). Morphology and microtubule organization in arabidopsis roots exposed to oryzalin or taxol. *Plant Cell Physiol.* **35**, 935-942.

Benfey, P. N., Linstead, P. J., Roberts, K., Schiefelbein, J. W., Hauser, M.-T. and Aeschbacher, R. A. (1993). Root development in Arabidopsis: four mutants with dramatically altered root morphogenesis. *Development* **119**, 1-14.

Beyer, E. M. Jr (1976). A potent inhibitor of ethylene action in plants. *Plant Physiol.* **58**, 268-271.

Bichet, A., Desnos, T., Turner, S., Grandjean, O. and Höfte, H. (2001). *BOTERO1* is required for normal orientation of cortical microtubules and anisotropic cell expansion in *Arabidopsis*. *Plant J.* **25**, 137-148.

Brown, R. M., Jr (1999) Cellulose structure and biosynthesis. *Pure Appl. Chem.* 71, 767-775.

Burk, D. H., Liu, B., Zhong, R. Q., Morrison, W. H. and Ye, Z. H. (2001). A katanin-like protein regulates normal cell wall biosynthesis and cell elongation. *Plant Cell* **13**, 807-827.

Carlemalm, E., Garavito, R. M. and Villiger, W. (1982). Resin development for electron microscopy and an analysis of embedding at low temperature. *J. Microsc.* **126**, 123-143.

Cosgrove, D. J. (1997). Relaxation in a high-stress environment: The molecular bases of extensible cell walls and cell enlargement. *Plant Cell* **9**, 1031-1041.

Fabri, C. O. and Schäffner, A. R. (1994). An Arabidopsis thaliana RFLP mapping set to localize mutations to chromosomal regions. *Plant J.* **5**, 149-156.

Fagard, M., Desnos, T., Desprez, T., Goubet, F., Refregier, G., Mouille, G., McCann, M., Rayon, C., Vernhettes, S. and Höfte, H. (2000). *PROCUSTE1* encodes a cellulose synthase required for normal cell elongation specifically in roots and dark-grown hypocotyls of arabidopsis. *Plant Cell* **12**, 2409-2423.

Fowke, L., Dibbayawan, T., Schwartz, O., Harper, J. and Overall, R. (1999). Combined immunofluorescence and field emission scanning electron microscope study of plasma membrane-associated organelles in highly vacuolated suspensor cells of white spruce somatic embryos. *Cell Biol. Int.* **23**, 389-397.

Furutani, I., Watanabe, Y., Prieto, R., Masukawa, M., Suzuki, K., Naoi, K., Thitamadee, S., Shikanai, T. and Hashimoto, T. (2000). The *SPIRAL* genes are required for directional central of cell elongation in *Arabidopsis thaliana*. *Development* **127**, 4443-4453.

Green, P. B. (1980). Organogenesis – a biophysical view. *Annu. Rev. Plant Physiol.* **31**, 51-82.

Hauser, M. T., Morikami, A. and Benfey, P. N. (1995). Conditional root expansion mutants of *Arabidopsis*. *Development* **121**, 1237-1252.

Hogetsu, T., Shibaoka, H. and Shimokoriyama, M. (1974). Involvement of cellulose synthesis in actions of gibberellin and kenetin on cell expansion. 2,6-Dichlorobenzonitrile as a new cellulose-synthesis inhibitor. *Plant Cell Physiol.* **15**, 389-393.

Holding, D. R., McKenzie, R. J. and Coomber, S. A. (1994). Genetic and structural analysis of five arabidopsis mutants with abnormal root morphology generated by the seed transformation method. *Ann. Bot.* **74**, 193-204.

Koornneef, M. and Stam, P. (1992). Genetic analysis. In: *Methods in Arabidopsis Research* (ed. C. Koncz, N. H. Chua and J. Schell), pp. 83-99. Singapore: World Scientific.

Lane, D. R., Wiedemeier, A., Peng, L. C., Höfte, H., Vernhettes, S., Desprez, T., Hocart, C. H., Birch, R. J., Baskin, T. I., Burn, J. E. et al. (2001). Temperature-sensitive alleles of *RSW2* link the KORRIGAN endo-1,4-β-glucanase to cellulose synthesis and cytokinesis in *Arabidopsis*. *Plant Physiol.* **126**, 278-288.

Liang, B. M., Dennings, A. M., Sharp, R. E. and Baskin, T. I. (1996). Consistent handedness of microtubule helical arrays in maize and *Arabidopis* primary roots. *Protoplasma* **190**, 8-15.

McClinton, R. S. and Sung, Z. R. (1997). Organization of cortical microtubules at the plasma membrane in arabidopsis. *Planta* **201**, 252-260.

Nicol, F., His, I., Jauneau, A., Vernhettes, S., Canut, H. and Höfte, H. (1998). A plasma membrane-bound putative endo-1,4-β-D-glucanase is required for normal wall assembly and cell elongation in *Arabidopsis*. *EMBO J.* **17**, 5563-5576.

Okuda, K. and Mizuta, S. (1987). Modification in cell shape unrelated to cellulose microfibril orientation in growing thallus cells of *Chaetomorpha moniligera*. *Plant Cell Physiol.* **28**, 461-473.

Peng, L. C., Hocart, C. H., Redmond, J. W. and Williamson, R. E. (2000). Fractionation of carbohydrates in *Arabidopsis* root cell walls shows that three radial swelling loci are specifically involved in cellulose production. *Planta* **211**, 406-414.

Preston, R. D. (1974). *The Physical Biology of Plant Cell Walls.* pp. 68-105. London: Chapman & Hall.

Sato, S., Kato, T., Kakegawa, K., Ishii, T., Liu, Y. G., Awano, T., Takabe, K., Nishiyama, Y., Kuga, S., Nakamura, Y. et al. (2001) Role of the putative membrane-bound endo-1,4-β-glucanase KORRIGAN in cell elongation and cellulose synthesis in *Arabidopsis thaliana*. *Plant Cell Physiol.* **42**, 251-263.

Scheres, B., di Laurenzio, L., Willemsen, V., Hauser, M. T., Janmaat, K., Weisbeek, P. and Benfey, P. N. (1995). Mutations affecting the radial organisation of the *Arabidopsis* root display specific defects throughout the embryonic axis. *Development* **121**, 53-62.

Schindelman, G., Morikami, A., Jung, J., Baskin, T. I., Carpita, N. C., Derbyshire, P., McCann, M. C. and Benfey, P. N. (2001) COBRA encodes a putative GPI-anchored protein, which is polarly localized and necessary for oriented cell expansion in Arabidopsis. *Genes Dev.* **15**, 1115-1127.

Sugimoto, K. (2000). *Cortical Microtubules, Cellulose Microfibrils and Growth Anisotropy in the Roots of* Arabidopsis thaliana. Ph. D. thesis, Australian National University, Canberra.

Sugimoto, K., Williamson, R. E. and Wasteneys, G. O. (2000). New techniques enable comparative analysis of microtubule orientation, wall texture, and growth rate in intact roots of arabidopsis. *Plant Physiol.* **124**, 1493-1506.

Sugimoto, K., Williamson, R. E. and Wasteneys, G. O. (2001). Wall architecture in the cellulose-deficient *rsw1* mutant of *Arabidopsis thaliana*: microfibrils but not microtubules lose their transverse alignment before microfibrils become unrecognizable in the mitotic and elongation zones of roots. *Protoplasma* **215**, 172-183.

Taiz, L. (1984). Plant cell expansion: regulation of cell wall mechanical properties. *Ann. Rev. Plant Physiol.* **35**, 585–657.

Thitamadee, S., Tuchihara, K. and Hashimoto, T. (2002) Microtubule basis for left-handed helical growth in arabidopsis. *Nature* **417**, 193-196.

Traas, J., Bellini, C., Nacry, P., Kronenberger, J., Bouchez, D. and Caboche, M. (1995). Normal differentiation patterns in plants lacking microtubular preprophase bands. *Nature* **375**, 676-677.

Tsuge, T., Tsukaya, H. and Uchimiya, H. (1996). Two independent and polarized processes of cell elongation regulate leaf blade expansion in *Arabidopsis thaliana* (L.) Heynh. *Development* **122**, 1589-1600.

Whittington, A. T., Vugrek., O., Wei, K. J., Hasenbein, N. G., Sugimoto, K., Rashbrooke, M. C. and Wasteneys, G. O. (2001). MOR1 is essential for organizing cortical microtubules in plants. *Nature* **411**, 610-613.

Williamson, R. E., Burn, J. E., Birch, R., Baskin, T. I., Arioli, T., Betzner, A. S. and Cork, A. (2001). Morphogenesis in *rsw1*, a cellulose-deficient mutant of *Arabidopsis thalania*. *Protoplasma* **215**, 116-127.

Wiedemeier, A. M. D. (1998). *Analysis of* Arabidopsis thaliana *Growth Anisotropy Mutants: Genetic, Physiological, and Cytological Characterization.* Ph. D. Thesis, University of Missouri, Columbia.